X-ray pump–Fluorescence imaging of reactive oxygen species for track analysis of synchrotron X-ray photoelectric nanoradiator dose

Jae-Kun Jeon [a], Jong-Ki Kim[a]*
[a]*Biomedical Engineering and Radiology, Catholic University of Daegu, School of Medicine, 33 Duryugongwonro17gil, Daegu,42472,* *Corresponding author: jkkim@cu.ac.kr

1. Introduction

Bursts of emissions of low-energy electrons, including interatomic Coulomb decay electrons and Auger electrons (0–1000 eV), as well as X-ray fluorescence produced by irradiation of large-Z element nanoparticles by either X-ray photons or high-energy ion beams, is referred to as the nanoradiator effect[1].

In therapeutic applications, this effect can damage pathological tissues that selectively take up the nanoparticles. Herein, a new nanoradiator dosimetry method is presented that uses probes for reactive oxygen species (ROS) incorporated into three-dimensional gels, on which macrophages containing either gold nanoparticles (AuNP) or iron oxide nanoparticles (IONs) are attached. Transport of nanoradiator dose was compared between two different nanoparticle system to investigate range of energy transfer through ROS [2].

2. Methods and Results

2.1 ROS gel

Gels containing the fluorescent probes, here termed ROS gels, were prepared by using agarose gel in a 1 ml tub, which was embedded in rubber clay, as shown in Fig. 1. Prior to gel formation, agarose solutions (0.2%) containing either 5 mM 2-[6-(40-amino)phenoxy-3H-xanthen-3-on-9-yl] benzoic acid (APF) or 100 mM hydroethidine-dihydroethidium (DHE) solution were magnetically stirred at 40 C in a nitrogen environment for mixing homogeneously. Macrophages were incubated with a 1 mg ml^{-1} solutions of either AuNP or IONs for 24 h in a Petri dish and then washed several times with the culture medium. The cells containing either AuNP or IONs were harvested and seeded again with the culture medium onto the surface of the agarose gel coated with poly l-lysine, and incubated for 24 h. After cell growth was confirmed by fluorescence microscopy, the gels (APF-AuNP, APF-ION, DHE-AuNP, DHE-ION) were mounted on the sample holder. Similar gel phantoms (i.e. without nanoparticle uptake; APF gel, DHE gel) were prepared for control experiments.

2.2 Synchrotron Irradiation on ROS gel

X-ray irradiation of a selected cell containing either AuNP or IONs was carried out in vacuo using synchrotron radiation at the PAL 4B bending-magnet beamline. The entire area of the selected cell was probed using a scanning polychromatic (5–14 keV) microbeam with a diameter of 5 mm. Since the typical size of the macrophage cell was estimated to be 10 mm, the X-ray beam scanned four times to cover the entire area of the cell. The radiation dose was measured with a UNIDOSE dosimeter using a Farmer-type chamber, and the total exposure was carried out for 3 s at a dose rate of 240 mGy s^{-1}. A cell selected in each ROS gel phantom (APF-AuNP, APF-ION, APF gel, DHE-AuNP, DHE-ION, DHE gel) was irradiated at the same position in the sample holder to ensure an identical environment of primary incidence X-rays.

2.3 Confocal microscopy imaging of ROS

This method, together with site specific irradiation of the intracellular nanoparticles from a microbeam of polychromatic synchrotron X-rays (5–14 keV), measures the range and distribution of OH radicals produced by X-ray emission or superoxide anions (O_2^-) produced by low-energy electrons. The measurements are based on confocal laser scanning of the fluorescence of the hydroxyl radical probe 2-[6- (40-amino)phenoxy-3H-xanthen-3-on-9-yl] benzoic acid (APF) or the superoxide probe hydroethidine-dihydroethidium (DHE) that was oxidized by each ROS, enabling tracking of the radiation dose emitted by the nanoradiator.

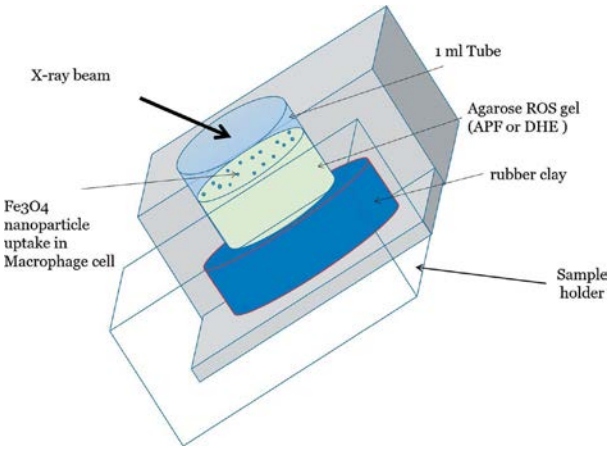

Fig. 1. ROS gel phantom for the measurement of X-ray photoelectric nanoradiator dose.

2.4 Results

In the range 900 μm below the irradiated cell, $OH^{\bullet}$ radicals derived mostly from either incident X-ray or X-ray fluorescence of either Au or ION nanoradiators are distributed along the line of incident direction in ROS gel. In contrast, O_2^- derived from secondary electron or low-energy electron emission by nanoradiators are scattered and distributed depth direction in the ROS gel. ROS fluorescence due to the nanoradiators was observed continuously to a depth of 1.5 mm for both Au and ION nanoradiators with APF

and DHE fluorescence, much longer with relatively larger intensity compared with the fluorescence track caused by the ROS produced solely by incident primary X-rays, which was limited to a depth of 600 mm, suggesting dose enhancement as well as more penetration by nanoradiators. Au-nanoradiator demonstrated relatively larger ROS intensity along the track compared with ION-nanoradiator, indicating more release of dose.

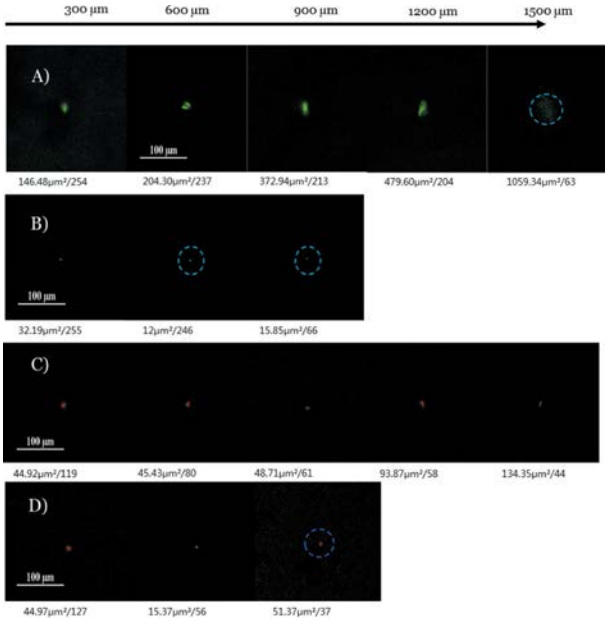

Fig. 2. Images of ROS fluorescence in each 3D ION-ROS gel section for $OH^{\bullet}$ (a) and O_2^- (c) produced, respectively, by ION-nanoradiators. Fluorescence images of (c) hydroxyl radicals and (d) superoxide produced by incident primary X-rays in an aqueous environment.

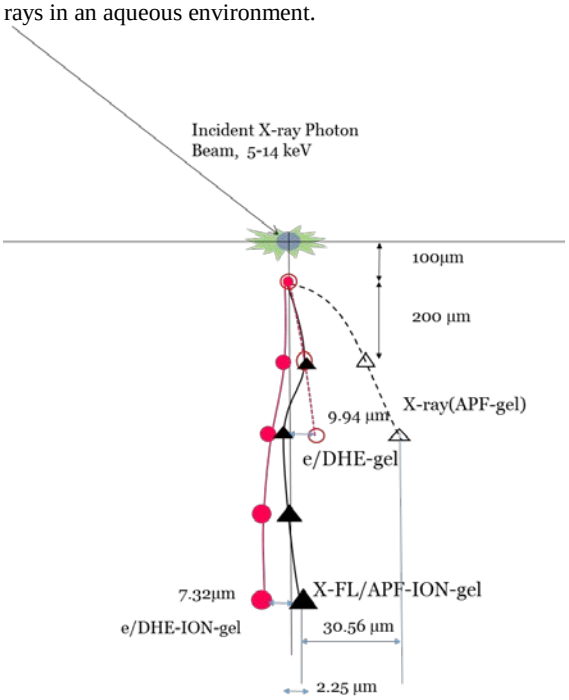

Fig. 3. Tracks of the radiation emitted by the nanoradiator along the depth of the ION-ROS gel showing different depths and angular directions of penetration of X-rays and low-energy electrons.

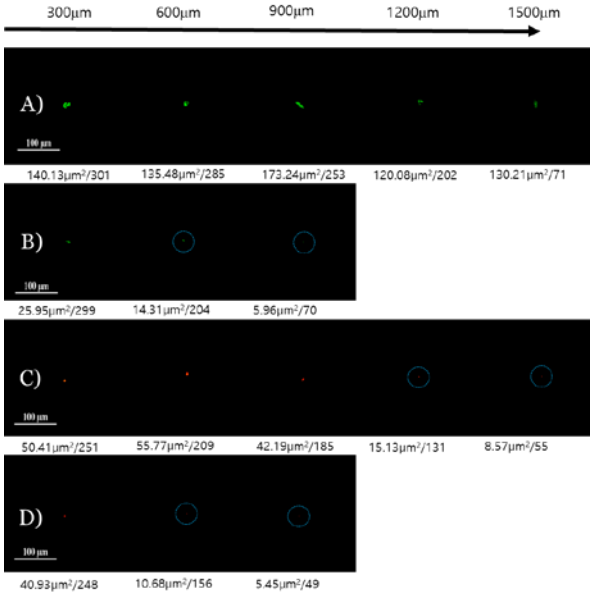

Fig.4. Images of ROS fluorescence in each 3D AuNP-ROS gel section for the hydroxyl radical (a,b) and superoxide (c,d) produced from AuNP nanoradiator, respectively.

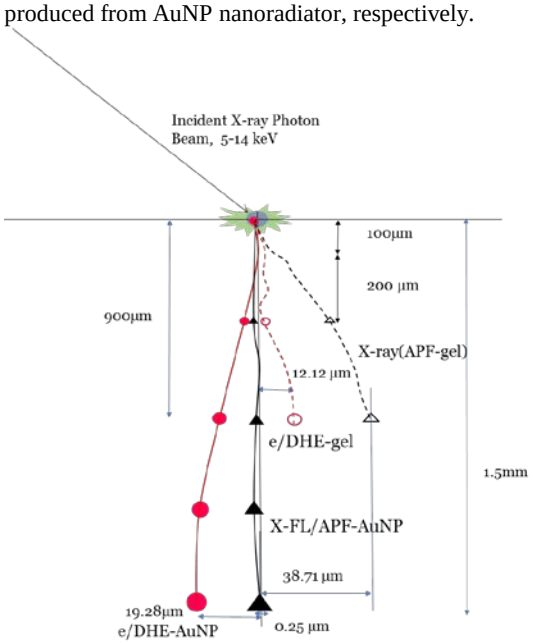

Fig.5. Tracks of the radiation emitted by the nanoradiator along the depth of the AuNP-ROS gel showing different depths and angular directions of penetration of X-rays and low-energy electrons.

3. Conclusions

the combined use of a synchrotron X-ray microbeam-irradiated three-dimensional ROS gel and confocal laser scanning fluorescence microscopy provides a simple dosimetry method for track analysis of X-ray photoelectric nanoradiator radiation, suggesting extensive cellular damage with dose-enhancement beyond a single cell containing IONs.

REFERENCES

[1] Kim, J.-K., Seo, S.-J., Kim, H.-T., Kim, K.-H., Chung, M.-H., Kim, K.-R. & Ye, S.-J. (2012). Phys. Med. Biol. 57, 8309–8323.
[2] Jeon J-K, Han S-M and Kim J-K, J. Synchrotron Rad. (2016). 23, 1191–1196.